z-scan like results produced by linear optical approximation of a nonlinear material

Rafael Quintero-Torres[1] and Lucila Zambrano-Valencia[2]
Departamento de Electrónica, Universidad Autónoma Metropolitana-Azcapotzalco
Av. San Pablo # 180, Col. Reynosa Tamaulipas, 02200 México, D.F., Mexico
e-mail:[1] rquintero@correo.azc.uam.mx; [2] lzv@correo.azc.uam.mx

Rosa María Bermúdez-Cruz
Departamento de Genética y Biología Molecular
Centro de Investigación y Estudios Avanzados del Instituto Politécnico Nacional
Av. Instituto Politécnico Nacional # 2508, 07360 México, D.F., Mexico
e-mail:roberm@gene.cinvestav.mx

Mrinal Thakur
Mechanical Engineering, Auburn University
Auburn AL 36849, USA
e-mail:mthakur@eng.auburn.edu

Recibido el 25 de mayo de 2000; aceptado el 13 de julio de 2000

A geometric optics procedure is developed to understand the nonlinear optical effects of materials, and to obtain z-scan like results. The change in the refractive index due to the optical nonlinearity is represented as a spherical lens. Thin and thick sample cases relative to the confocal length, defined by an external lens are modeled. Linear and nonlinear absorption is included in material with instantaneous nonlinear response, slow response mechanisms like thermal effect can be included. With this procedure an explanation for the distortion in the z-scan is obtained with the increase in the aperture, the nonlinear refractive index and the sample thickness as well as with the presence of nonlinear absorption.

Keywords: z-scan; nonlinear refractive index; nonlinear absorption

Se emplea óptica geométrica para entender el efecto óptico no lineal en materiales y obtener resultados que se asemejan al barrido en z. El cambio en el índice de refracción debido a la no linealidad óptica se representa como una lente esférica. Se discute el caso de muestras delgadas y gruesas (el espesor de la muestra se mide respecto a la distancia confocal definida por la lente externa). La absorción lineal y no lineal se incluyen en materiales con respuesta no lineal instantánea, de la misma manera se pueden considerar mecanismos de respuesta lenta como los térmicos. Esta interpretación da cuenta de la deformación de los resultados del barrido en z al aumentar la apertura, los efectos no lineales, el espesor y la absorción.

Descriptores: Barrido en z; índice de refracción no lineal; absorción no lineal

PACS: 78.20.Ci; 42.65.-k; 42.70.-a

1. Introduction

Nonlinear optics is becoming one of the most important branches of modern optics due to its tremendous impact in the electronics technology. Some examples of applications where nonlinear optical phenomenon is playing a mayor role are frequency conversion, optical modulation, optical switching, optical gates and optical memories, among others.

Nonlinear optical phenomenon is shown basically in all materials. Non linearity is a property of the medium rather than a property of light. Optical effects are overdriven into nonlinear effects when light of high intensity is present in an optical medium. The intensity needed to observe these effects depends on the nature of the material. When ordinary light propagates through an optical material, the electric field $\mathbf{E}$ associated with the light beam exerts a polarizing force on the electrons of the material allowing mainly outer electrons to respond. The optical medium is polarized and this polarization is proportional to the applied electric field $\mathbf{E}$.

If the radiated field becomes large enough, to be comparable with the atomic fields, then proportionality begins to fail and the superposition principle does not apply any longer. Non linear phenomena are due to the inability of the dipoles to respond in a linear way when light of very large amplitude interacts with matter. It is customary to express the polarization $\mathbf{P}$ in a power series of $\mathbf{E}$, where ξ represents the susceptibility:

$$\mathbf{P} = \xi^{(1)} \cdot \mathbf{E} + \xi^{(2)} : \mathbf{EE} + \xi^{(3)} : \mathbf{EEE} + \ldots \qquad (1)$$

The search of new and more efficient materials and devices to be used in electronic systems shows continuous growth. The quest for experimental techniques to determine properties, where simplicity and usefulness was sought, per-

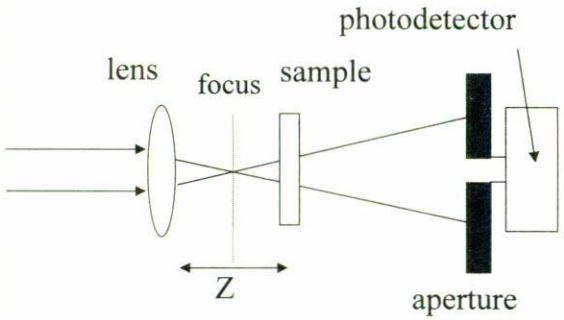

FIGURE 1. z-scan experimental arrangement, the lens defines the focus and the sample is scanned through z near the focus.

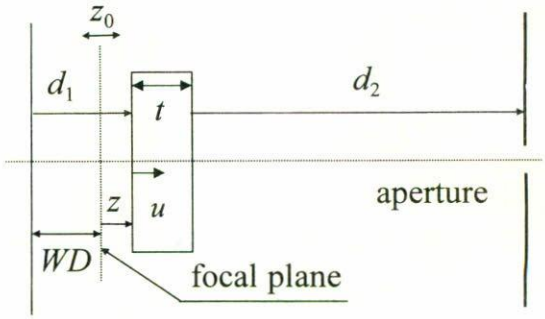

FIGURE 2. Geometrical definition, the focal plane is defined by the external lens, z_0 is the confocal length and t is the sample thickness.

mitted the development of the so called z-scan technique [1], used to measure nonlinear refractive index and nonlinear absorption. In this technique, a thin sample is scanned through the focus of a gaussian laser beam, where light can pass from side to side of the sample with small distortion of the wave front. A sensor is placed behind a finite aperture in the far field to monitor the output of the sample (Fig. 1). The experimental arrangement is set in a way that a single beam and a single path of light is used to determine the nonlinear refractive index and the nonlinear absorption. It is possible to achieve temporal resolution if a Michelson interferometer is used before the z-scan arrangement to produce one path-two beams [2] experiment, using the delay arm in the interferometer to produce autocorrelation, constant average power and variable peak power.

Starting the scan near the lens (far from focus), the intensity is low and the transmittance through the aperture is constant. As the sample comes nearer to the focus, the intensity becomes larger and a self-focusing effect is observed (case of positive nonlinear refractive index). It makes the beam to collimate resulting in an increase in the transmittance. When the sample goes beyond the focal plane, a self-defocusing occurs leading a beam broadening at the aperture and the transmittance decreases (the opposite is obtained when material used has a negative nonlinear refractive index). Similar conclusions have been reached for the z-scan signature, when different considerations were taken [3, 4].

2. z-scan results

In this section, we present the results obtained with the z-scan technique and it is compared with results obtained when the geometric optics technique is used. In the original z-scan work, a simplification of the normalized on-axis z-scan transmittance is derived considering small nonlinearities, $|\Delta\Phi| \ll 1$, where the phase change for the wave after the material ($\Delta\Phi = 2\pi n_2 I_0 t/\lambda$) is defined by the nonlinear refraction index n_2, the intensity I_0, the thickness t and the wavelength used λ. A far field condition was used, with the aperture positioned at several times the confocal length z_0 apart from the focus, where the confocal length ($z_0 = \pi\omega_0^2/\lambda$) is defined with as the minimum spot radius produced by the focusing lens. And measuring the transmission only when the sample is close to the focal point, $|z| \cong z_0$. A small aperture is used ($s \to 0$), s indicates the percentage of light that passed the aperture, producing the next set of equations, where T stands for transmission as a function of the z position and the phase change $\Delta\Phi$ due to the material, x is the normalized position. ΔZ_{p-v} is the distance between the peak and the valley in the z-scan signature. ΔT_{p-v} is the transmission difference between the peak and the valley in the z-scan:

$$T(z, \Delta\Phi) \approx 1 + \frac{4\Delta\Phi x}{(x^2+9)(x^2+1)}, \tag{2}$$

$$x = \frac{z}{z_0}, \tag{3}$$

$$\Delta Z_{p-v} \sim 1.7 z_0, \tag{4}$$

$$\Delta T_{p-v} \sim 0.406\Delta\Phi. \tag{5}$$

The variables used in this work are defined in Fig. 2, where the sample position from the focal plane is $z = d_1 - WD$ and the distance from the focal plane to the aperture is $B = z + d_2 + t$. The far field condition is represented by $B \gg z_0$, the inclusion of a thick sample changes de focal plane significantly and the need of an absolute fix position is solved with the use of the lens working distance WD.

3. Geometric optics approximation

Two general cases are considered in this work; in the first case, a thin sample of nonlinear optical material is modeled as a linear optical element with properties dependent on the intensity and in the second case, thick samples are modeled as a set of slices, each one with a fraction of the effect. In both cases, transparent or absorbing materials are assumed. In this section we describe the steps of the procedure that are common to both cases.

In the derivation of the geometrical optics technique, the complex beam radius [5, 6] $q(z)$ is used to study the propagation of the gaussian beam through a nonlinear medium. This radius is represented by the known expression

$$\frac{1}{q(z)} = \frac{1}{R(z)} - \frac{i\lambda}{\pi\omega^2(z)n}, \tag{6}$$

where $R(z)$ is the wavefront radius of curvature and $\omega(z)$ is the beam radius.

The basic question to solve is: how does the gaussian beam $q(z)$ change as it passes through a nonlinear plate? In other words, how does the transmission through an aperture at far field change when the sample moves near the focal plane?

The geometric optics approximation technique is based on the assumption that a change in the refractive index takes place $(n + \Delta n)$ when a laser beam (source of high-intensity coherent light) impinges on a nonlinear material. This change due to the light intensity is directly related to the electronic interaction or indirectly related to thermal effects and follows the intensity distribution of the light, in this case a gaussian shape or the temperature distribution. Considering the trajectory of the light, it is equivalent to consider a parallel plate with a refractive index function of the position z and r, or a material with a uniform refractive index n with a non parallel plate, rather a geometrical shape resembling the plate plus a gaussian deformation. Ideally, a gaussian lens should be added or subtracted to the sample, however the simplicity of this approximation consists in the use of a spherical lens instead.

The intensity distribution for the Gaussian beam at radius r and position z, $I(r, z)$ is represented in the next equation, where the intensity at focus, $r = 0$ and $z = 0$ is I_0:

$$I(r, z) = I_{\text{axis}} \exp\left[-\frac{2r^2}{\omega^2(z)}\right], \tag{7}$$

$$I_{\text{axis}} = \frac{2P}{\pi\omega^2(z)} = I_0\left[1 + \left(\frac{z}{z_0}\right)^2\right]^{-1}. \tag{8}$$

Subsequently, finding an equation for the focal length of the spherical lens as a function of the nonlinear properties in the material and the intensity distribution $\omega(z)$, is possible. Following Fig. 3, lets assume that at $r = \omega$ the sphere touches the sample and also the radius of the sphere is bigger than the thickness of the sample $R > t\Delta n/n$, meaning that the nonlinear effect is small. From that it is easy to reach an expression for R:

$$R \approx \frac{\omega^2(z)n}{2tn_2 I(r, z)}. \tag{9}$$

The focal length of a lens is defined as the radius of the lens divided by the change in the refractive index produced by the lens:

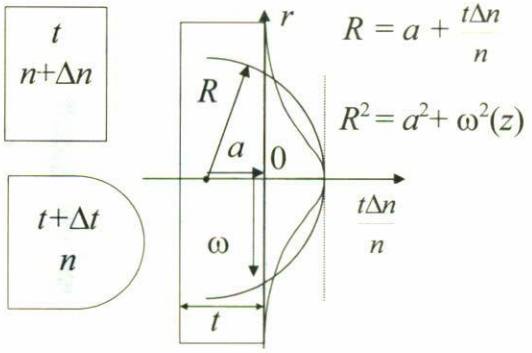

FIGURE 3. Contrasting a gaussian and a spherical function, to relate ω and R.

$$\begin{aligned}\frac{1}{f} &\equiv \frac{(n-1)}{R} \\ &= \frac{(n-1)2tn_2 I_{\text{axis}}\left[1 + \left(\frac{z}{z_0}\right)^2\right]^{-1}}{n\omega_0^2\left[1 + \left(\frac{z}{z_0}\right)^2\right]} \\ &= \left(\frac{n-1}{n}\right)\frac{\Delta\Phi}{z_0}\left[1 + \left(\frac{z}{z_0}\right)^2\right]^2,\end{aligned} \tag{10}$$

where

$$\Delta\Phi = \frac{2\pi n_2 I_0 t}{\lambda}. \tag{11}$$

In order to determine the change in the complex beam radius $q(z)$ at any point as a function of any optical element in the path, the use of an $ABCD$ matrix or transfer matrix will be used:

$$\text{output} = \begin{vmatrix} A & B \\ C & D \end{vmatrix} \text{ input}, \tag{12}$$

$$\frac{1}{q_{\text{output}}} = \frac{C + \left(\frac{D}{q_{\text{input}}}\right)}{A + \left(\frac{B}{q_{\text{input}}}\right)}, \tag{13}$$

where the matrix elements A, B, C, and D have information of all optical elements between the input and the output.

Next equation is a general expression for the change in the laser spot size with the information of Fig. 2:

$$\omega_{\text{out}}^2 = \omega_0^2\left[\frac{A^2 + \left(\frac{B - A\,WD}{z_0}\right)^2}{AD - BC}\right]. \tag{14}$$

The linear transmission through an aperture of radius a, T_L; is defined as the ratio of the power carried within the circle of radius a in the transverse plane at position z, $P(a)$, to the total power $P(r \to \infty)$. In the linear case, it is the constant s:

$$T_L(z) = \frac{P(a)}{P(r \to \infty)} = 1 - \exp\left[-\frac{2a^2}{\omega_L^2(z)}\right] \equiv s. \tag{15}$$

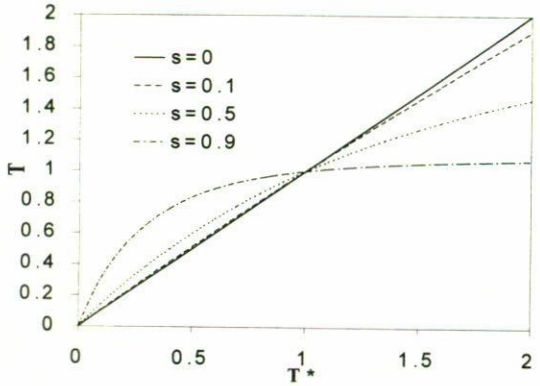

FIGURE 4. Typical z-scan transmission through different apertures s. Here the origin of the asymmetry in the z-scan is explicable.

Finally, T defines the transmission as the ratio between the power through the aperture due to a nonlinear system defined by an $ABCD$ matrix and a linear system defined by other $ABCD$ matrix, (T_{NL}/T_L, this consideration will make the transmission equal to one when a linear material is used).

$$T \equiv \frac{T_{NL}(a)}{T_L(a)} = \frac{\left[1-(1-s)^{\frac{\omega_L^2(z)}{\omega_{NL}^2(z)}}\right]}{s}, \tag{16}$$

$$T^* \equiv \lim_{x\to 0} T = \frac{\omega_L^2(z)}{\omega_{NL}^2(z)}. \tag{17}$$

Figure 4 shows the aperture effect [Eq. (16)], and indicates that when $s \to 1$ (large aperture) the z-scan transmission greater than one goes faster to 1 than the z-scan transmission smaller than one; that is, the aperture will affect the symmetry in z-scan, shrinking the positive hump faster than the negative one. This information is useful because many solids are not perfectly homogeneous and a larger aperture is needed to produce a meaningful result.

4. Thin transparent sample analysis, thickness smaller than the confocal length, $t < z_0$

A set of equations for typical z-scan conditions where a, thin sample with $t \ll z_0$ and intensity small enough such that $\Delta\Phi \ll 1$, can be obtained if the $ABCD$ matrix for the linear system and for the nonlinear system are defined and from them the ω_{out} is determined.

The $ABCD$ matrix that characterizes a linear system propagating through air with

$$\text{input}\,|\leftarrow d_1 \rightarrow\leftarrow d_2 \rightarrow|\,\text{output},$$

is expressed

$$\begin{vmatrix} A & B \\ C & D \end{vmatrix} = \begin{vmatrix} 1 & d_1+d_2 \\ 0 & 1 \end{vmatrix}. \tag{18}$$

where only two propagations d_1 and d_2 are needed.

The expression of the $ABCD$ matrix for a nonlinear system is

$$\begin{vmatrix} A & B \\ C & D \end{vmatrix} = \begin{vmatrix} 1-\dfrac{d_2}{f} & d_1+d_2-\dfrac{d_1 d_2}{f} \\ -\dfrac{1}{f} & 1-\dfrac{d_1}{f} \end{vmatrix}, \tag{19}$$

in this case

$$\text{input}\,|\leftarrow d_1 \rightarrow \text{O} \leftarrow d_2 \rightarrow|\,\text{output},$$

indicates the need to use two propagations d_1, d_2 and the nonlinear effect represented by only one ideal variable thin lens (O).

To obtain the transmission equation, we substitute the last two $ABCD$ equations in Eq. (14) in order to obtain the laser spot size for a linear and a nonlinear system respectively, and then substituting in Eq. (17) to end up with:

$$T^* = \frac{\omega_L^2(z)}{\omega_{NL}^2(z)} = \frac{z_0^2+(z+d_2)^2}{\left[z_0\left(1-\dfrac{d_2}{f}\right)\right]^2+\left[d_2+z\left(1-\dfrac{d_2}{f}\right)\right]^2}. \tag{20}$$

Simplifying this equation with the far field condition, $d_2 \gg z_0$ and the expression for the focal length [Eq. (10)], will produce the set of expected equations:

$$T^*(z,\Delta\Phi) \approx 1+\left(\frac{n-1}{n}\right)\frac{2\Delta\Phi x}{(x^2+1)^2},$$

$$x = \frac{z}{z_0}, \tag{21}$$

$$\Delta Z_{p-v} \cong \frac{2}{\sqrt{3}} z_0, \tag{22}$$

$$\Delta T^*_{p-v} \cong \frac{9}{8}\left(\frac{n-1}{n}\right)\Delta\Phi \approx 0.75\Delta\Phi. \tag{23}$$

5. Thick samples analysis, thickness larger than the confocal length ($t > z_0$), with linear and nonlinear absorption

This case is a generalization of the thin sample case where $t > z_0$ and or $\Delta\Phi \gg 0$. In this procedure, multiple nonlinear lenses replace the single nonlinear lens to keep the local situation inside the scope of the previous case. The amount of lenses is defined by the thickness and the intensity. Now a new situation is taken into account, the power inside the sample decreases due to linear and nonlinear absorption, this absorption is intensity-dependent.

For this case the intensity is not a good number because of the variation in the spot area, therefore a better one is the power (P) and the general equation to find the power is a

function of the linear absorption α and the nonlinear absorption β, where $\beta I(u)$ is the change in absorption due to the intensity ($\Delta\alpha$):

$$\frac{dP}{du} = -[\alpha + \beta I(u)]P. \tag{24}$$

Where the power inside the sample as a function of internal length l is

$$\frac{1}{P(u)} = \frac{1}{T_1 P_0}\exp(\alpha u) - \frac{m}{\alpha + p}\exp(\alpha u) \times [\exp(-\alpha u - k|c+u|) - \exp(-k|c|)], \tag{25}$$

$$m = \frac{2\beta}{\pi\omega_0^2},$$

$$c = (d - WD)n,$$

$$k = \frac{1}{2}\ln\left(1 + \frac{4}{n^2 z_0^2}\right), \tag{26}$$

where n, T_1, P_0 represent refractive index, incident surface transmission and incident power respectively. To end up with an elemental function, it was needed to change the variation in the radius with an exponential variation as follows:

$$\frac{a}{b + (c+u)^2} \approx m\exp(-k|c+u|). \tag{27}$$

When the area is uniform ($k = 0$), the result for absorption in a waveguide is recovered [7]:

$$\frac{1}{I(u)} = \exp(\alpha u)\left\{\frac{\beta}{\alpha}[1 - \exp(-\alpha u)] + \frac{1}{T_1 I_0}\right\}. \tag{28}$$

For the thick film, the nonlinear material is substituted by a set of slices of the same material, where each one can be modeled as a "nonlinear lens". The explicit $ABCD$ matrix elements defining a linear thick system

$$\text{input}\,|\leftarrow d_1 \rightarrow |t| \leftarrow d_2 \rightarrow |\,\text{output},$$

is

$$\begin{vmatrix} A & B \\ C & D \end{vmatrix} = \begin{vmatrix} 1 & d_1 + d_2 + \frac{t}{n} \\ 0 & 1 \end{vmatrix} \tag{29}$$

where $|t|$ represents the sample thickness.

The nonlinear system over the same path is schematically represented with

$$\text{input}\,|\leftarrow d_1 \rightarrow []\text{O}[]\text{O}\ldots[]\text{O} \leftarrow d_2 \rightarrow |\,\text{output},$$

and

$$\begin{vmatrix} A & B \\ C & D \end{vmatrix} = \begin{vmatrix} 1 & d_2 \\ 0 & 1 \end{vmatrix} \begin{vmatrix} 1 & \frac{\delta}{n} \\ -\frac{1}{f_i} & 1 - \frac{\delta}{f_i n} \end{vmatrix} \begin{vmatrix} 1 & \frac{\delta}{n} \\ -\frac{1}{f_{i-1}} & 1 - \frac{\delta}{f_{i-1} n} \end{vmatrix} \cdots \begin{vmatrix} 1 & \frac{\delta}{n} \\ -\frac{1}{f_1} & 1 - \frac{\delta}{f_1 n} \end{vmatrix} \begin{vmatrix} 1 & d_1 \\ 0 & 1 \end{vmatrix} \tag{30}$$

all optical elements are included. [ ] represents a slice of linear material and O represents an ideal nonlinear lens associated with that slice.

The $ABCD$ elements for the nonlinear part are obtained from multiplication of all matrices. The explicit forms for each A, B, C and D for m elements are shown in Eq. (31) where i goes from 1 to m.

$$\begin{aligned}
A &= A_i, \\
A_i &= A_{m-i+1}\left(1 - \frac{\delta}{n f_{m-i+1}}\right) + \frac{B_{m-i+1}}{f_{m-i+1}}, \\
A_0 &= 1, \\
B &= A_i d_1 + B_1, \\
B_i &= A_{m-i+1}\left(\frac{\delta}{n}\right) + B_{m-i+1}, \\
B_0 &= d_2, \\
C &= C_i, \\
C_i &= C_{m-i+1}\left(1 - \frac{\delta}{n f_{m-i+1}}\right) + \frac{D_{m-i+1}}{f_{m-i+1}}, \\
C_0 &= 0, \\
D &= C_i d_1 + D_1, \\
D_i &= C_{m-i+1}\left(\frac{\delta}{n}\right) + D_{m-i+1}, \\
D_0 &= 1.
\end{aligned} \tag{31}$$

To implement those expansions is simple, and a sequence is outlined next:

- From the original conditions define the amount of elements to use. If $t > \omega_0$ the number of elements is t/ω_0 and the slice thickness δ = (sample thickness)/(number of elements).
- Calculate P at each element using Eq. (25) as a function of d_1. d_1 is now a better reference than $z = 0$ because it is absolute. The change in $z = 0$ relative to the physical equipment is due to a focal plane change as the sample moves around it. However this shift can be calculated at any particular situation.

TABLE I. Parameters used in the simulation of Figs. 5 and 6.

λ	$1.064\,\mu$m	α	$0.6\ \text{cm}^{-1}$
d_2	$100\,z_0$	β	0.05 cm/MW
n	1.86	P_0	5 W
n_2	$-1\times10^{-5}\ \text{cm}^2$/MW	s	0.5
z_0	$47.24\,\mu$m	ω_0	$4\,\mu$m

- Calculate f for each element Eq. (10).
- Calculate $ABCD$ using Eq. (31).
- Calculate ω's using Eq. (14).
- Calculate T_A [Eq. (17)], it is identified with the A subindex because now the absorption effect is included in the focal length calculation. Calculate the total power transmitted by the sample (T_P), that measures the transmission without the aperture ($s \to 1$), and it is the ratio between total output power (P_{output}) and input power (P_0). The normalized transmission through the sample in a z-scan experiment is the multiplication of T_A and T_P; and this is called the real transmission (T_{REAL}). (T_{REAL}) represents the output signal in an actual z-scan experiment with an aperture (used to measure nonlinear refractive index); T_P represents the output signal in an actual z-scan experiment with no aperture (used to measure nonlinear absorption).

$$\mathrm{T}_{\text{REAL}} = \mathrm{T}_A \frac{P_{\text{output}}}{P_0} = \mathrm{T}_A \mathrm{T}_p. \qquad (32)$$

- Finish the scan, changing d_1.

Table I includes the parameters(8) used to obtain Figs. 5 and 6. Figure 5 show $\mathrm{T}^*(s \to 0)$, the ideal z-scan transmission removing the aperture effect and the linear and nonlinear effect; $\mathrm{T}(s = 0.5)$, the z-scan transmission modified by the aperture effect; $\mathrm{T}_{\text{REAL}}(s = 0.5, \alpha \neq 0, \beta \neq 0)$ represents an expected actual experimental z-scan results to see the refractive index and $\mathrm{T}_P(s \to \infty, \alpha \neq 0, \beta \neq 0)$ represents an expected actual experimental z-scan results to see the nonlinear absorption. All these variables were calculated in samples with a thickness of 10 μm, 100 μm and 600 μm respectively. From them it is possible to see the thickness effect (because $z_0 \sim 50\,\mu$m), the effect due to absorption and the consequence of the aperture size. T^* and T are equal to one when the sample is far from the high intensity zone. The linear absorption in the material decreases T_{REAL} values and the overall effect, as was expected. The magnitude of the nonlinearities measured by peak to valley transmission is smaller in the thin sample. Figure 5c shows that a thick sample ($t > z_0$) will have the distance between peak and valley position related to the thickness ($\Delta Z_{p-v} \sim t/n$) rather than to the confocal length.

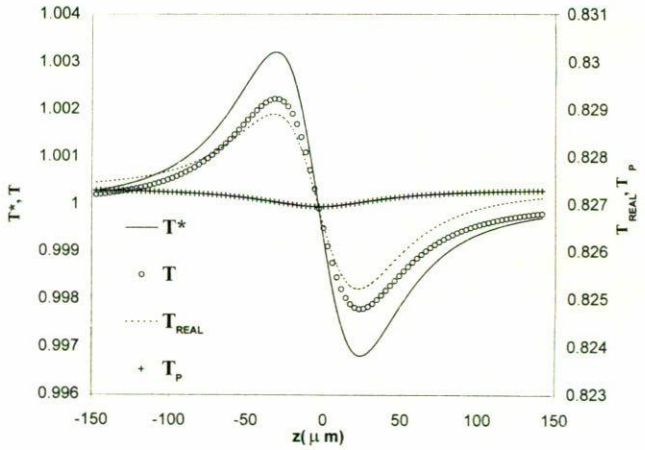

(a)

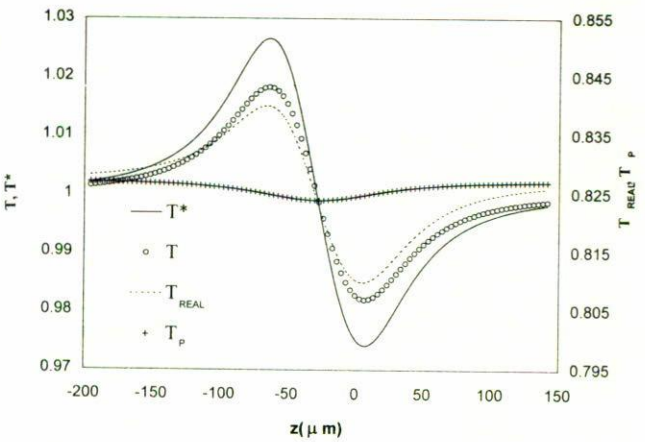

(b)

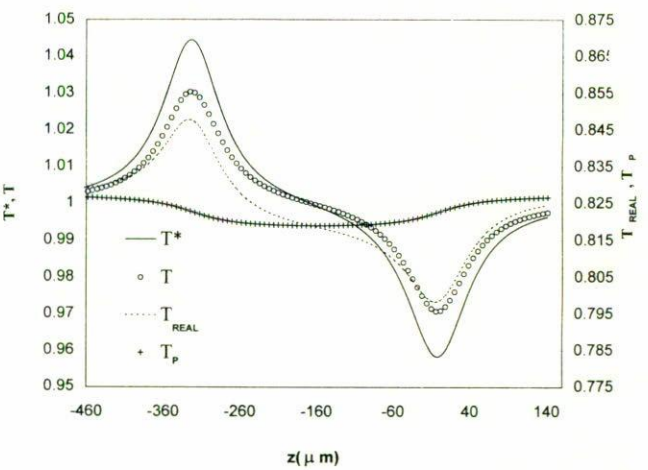

(c)

FIGURE 5. a) z-scan transmission for a sample with a thickness of (a) 10 μm, (b) 100 μm and (c) 600 μm, and a confocal length of 47.24 μm.

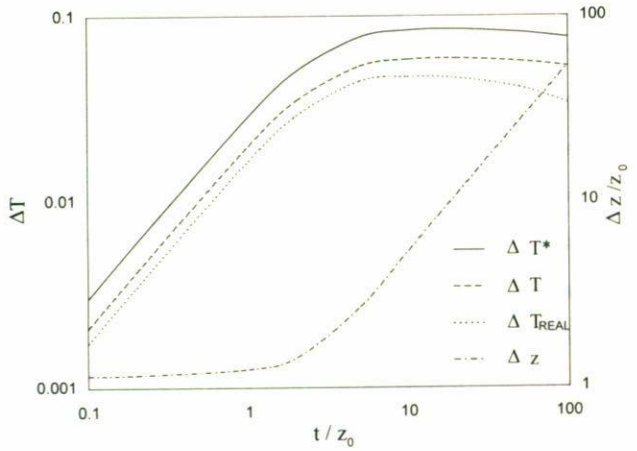

FIGURE 6. Three plots for the change in transmission as a function of the thickness, ideal (T^*), aperture $s = 0.5$ (T), and absorption different from cero (T_{REAL}). One plot for the change in the distance between peal and valley, the result is approximately the same for the three cases.

Figure 6 shows four plots as a function of sample thickness, from 10 times smaller than the confocal length to 100 times the confocal length. ΔT_{p-v} measures the maximum transmission T_{peak}, minus minimum transmission $T_{valley}(s \to 0)$. Similar definitions stand for $T^*(s = 0.5)$, and for $T_{REAL}(s = 0.5, \alpha \neq 0, \beta \neq 0)$. Here it is possible to see linear increase of the phase change as the thickness increases and saturates for thickness larger than the confocal length. For T_{REAL} the confocal length decreases when the thickness increases due to the absorption or if the incident power is high enough. In the right Y-axis the change in z distance between peak and valley is shown as a function of sample thickness. For thickness larger than the confocal length a linear increase can be seen, for thin samples this is a constant value and proportional to the confocal length. The difference between standard ($t \ll z_0$) and extended ($t > z_0$) z-scan is clear.

6. Summary

A simple review of classical optics is useful to describe a powerful technique with widespread use to characterize nonlinear materials. The well known results are reproduced and generalizations toward less common conditions were provided; they are useful mainly in solids where the sample conditions or the laser characteristics are not always under control. An added gain is the insight in the experimental arrangement than can be obtained by analyzing the geometry effects. This work is illustrated with simulated results from a nonlinear material to discuss the interrelation between the technique arrangements, the experimental results and the material properties.

Acknowledgments

This project was supported by a grant from National Council of Science and Technology from Mexico (CONACyT), under project 29032-A.

1. M. Sheik-Bahae *et al.*, *IEEE J Quantum Electronics* **26** (1990) 760, and references therein).
2. R. Quintero-Torres and M. Thakur, *Appl. Phys. Lett.* **66** (1995) 1310.
3. M. Sheik-Bahae *et al.*, *Optical Engineering* **30** (1991) 1228.
4. J.A. Hermann and R.G. McDuff, *J. Opt. Soc. Am. B.* **10** (1993) 2056.
5. A.E. Siegman, *Lasers*, (University Science Books, Mill Valley, Calif., 1986).
6. A. Yariv, *Optical Electronics*, (Holt, Rinehart and Winston, New York, 1976).
7. L.A. Hornak, *Polymers for Lightwave and Integrated Optics: Technology and Applications*, (Marcel Dekker, Inc, New York, 1992).
8. R. Quintero-Torres and M. Thakur, *J. Appl. Phys.* **85** (1999) 401.